A Novel Hybrid Inorganic–Metalorganic Compound Based on a Polymeric Polyoxometalate and a Copper Complex: Synthesis, Crystal Structure and Topological Studies

Leire San Felices, Pablo Vitoria, Juan M. Gutiérrez-Zorrilla,* Santiago Reinoso, Juan Etxebarria, and Luis Lezama[a]

Abstract: Reaction of monosubstituted Keggin polyoxometalates (POMs) and $[Cu(ac)(pmdien)]^+$ generated in situ led to the formation of the hybrid metal organic–inorganic compound $K_5[Cu(ac)(pmdien)][SiW_{11}CuO_{39}]\cdot 12H_2O$; its crystal structure and magnetic properties have also been determined. The packing of this compound can be viewed as a stacking of hydrogen-bonded chiral double chains, with the cationic complexes located between the two-dimensional arrangement of POM double chains. DFT calculations performed on $[Cu(ac)(pmdien)]^+$ suggest that the distortion presented in this cationic copper complex is due to electronic effects. An AIM stability study of the cationic copper complex, in order to determine the relationship between the bond angle Cu-O-C and the denticity of the acetate ligand, has been carried out. Topological analyses over the polyhedral distortion, both of the monosubstituted polyanion and copper complexes, have been performed by means of continuous shape measures (CSM).

Keywords: copper complexes · density functional calculations · polyhedral distortion · polyoxometalates

Introduction

Polyoxometalates (POMs)[1] form a large and characteristic class of inorganic compounds of incomparable electronic versatility and structural diversity that have attracted great attention due to their utility in chemistry,[2] catalysis,[3] material science[4] and medicine.[5] All these reflect a current interest in assembling different inorganic and metal–organic building blocks in order to produce hybrid compounds that combine the different characteristics of the components to obtain unusual structures or properties. Recently, several hybrid compounds based on vanadium and molybdenum isopolyanions have been reported.[6] However, hybrid supramolecular arrays based on Keggin-type POM and derivatives as the inorganic component, have not been extensively studied.[7] Structures of extended Keggin heteropolyanions have been observed only in monosubstituted derivatives of manganese: $(ET)_8[PW_{11}MnO_{39}]\cdot 2H_2O$;[8] cobalt: $(Et_3NH)_5[XW_{11}CoO_{39}]\cdot 3H_2O$ (X: P, As)[9] and $[Co(dpa)_2(H_2O)_2]_2(Hdpa)$ $[PW_{11}CoO_{39}]\cdot 3H_2O$;[10] and copper: $[Cu(en)_2(H_2O)]_2[\{Cu(en)_2\}_2SiW_{11}CuO_{39}]\cdot 3H_2O$.[11]

Our interest is focused on the preparation of new hybrid compounds by assembling monosubstituted Keggin POMs and transition metal carboxylate complexes.[12] In order to rationalize the influence of various TM–carboxylate complexes on the formation of monosubstituted Keggin POM–-metal organic hybrid compounds, we studied the reactivity of different carboxylate amine copper complexes. This study includes the binuclear Cu-bpy-ox and Cu-phen-ox complexes and mononuclear Cu-dien-ac and Cu-pmdien-ac complexes. In this paper we report the synthesis, crystal structure and magnetic properties of the compound $K_5[Cu(ac)(pmdien)][SiW_{11}CuO_{39}]\cdot 12H_2O$, **1**, (ac: acetate; pmdien: *N*,*N*,*N*′,*N*″,*N*″-pentamethyldiethylentriamine) together with a topological analysis of the polyhedral distortion by using continuous shape measures (CSM) and an AIM stability study of the cationic copper complex. This has two purposes: first, to check the influence of packing in the complex geometry and second to determine the relationship between the bond angle Cu-O-C and the denticity of the acetate ligand.

[a] L. San Felices, P. Vitoria, Prof. Dr. J. M. Gutiérrez-Zorrilla, S. Reinoso, J. Etxebarria, Dr. L. Lezama
Departamento de Química Inorgánica
Facultad de Ciencia y Tecnología
Universidad del País Vasco, Apdo 644
48080 Bilbao (Spain)
E-mail: qipguloj@lg.ehu.es

Supporting information for this article is available on the WWW under http://www.chemeurj.org/ or from the author.

DOI: 10.1002/chem.200400279

Results and Discussion

Synthesis and chemical characterization: In contrast to most TM complex–POM hybrid compounds reported in the literature—which are synthesized by hydrothermal methods—we have made use of the classical open-air techniques for the preparation of these compounds. They are formed by autoassembly of the building blocks generated in situ. Compound **1** has been characterized by elemental analysis, FTIR spectroscopy and thermogravimetric analysis.

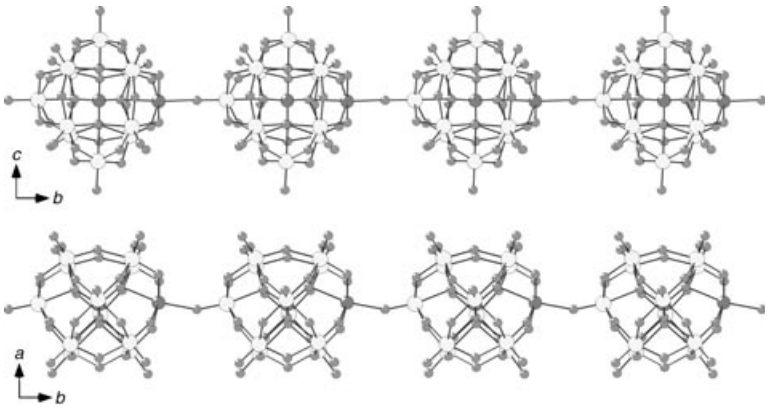

Figure 2. Views of the one-dimensional $[SiW_{11}CuO_{39}]_n^{6n-}$ chain running along the [010] direction.

The thermal decomposition of **1** takes place in four main stages, with the first three made of two overlapped steps. The water molecules are lost in the first endothermic stage (50–225 °C). The three remaining stages are exothermic processes related to organic component oxidations and POM structure breakdown (225–365 °C; 365–460 °C; 460–640 °C). The quantitative analysis by mass spectrometry of the gases evolved in the oxidation steps indicates a good agreement between the experimental and calculated carbon content present in the compound.

Description of crystal structure: The title compound crystallizes in the monoclinic space group $P2_1$ with one $[SiW_{11}CuO_{39}]^{6-}$, one $[Cu(ac)(pmdien)]^+$ cationic complex, five potassium cations and twelve water molecules in the asymmetric unit.

The $[SiW_{11}CuO_{39}]^{6-}$ α-Keggin unit consists of a central SiO_4 tetrahedron surrounded by four vertex-sharing M_3O_{13} trimers: one CuW_2O_{13} and three W_3O_{13} (Figure 1). The POMs share one oxygen atom bound to Cu1 and W11 atom to form the infinite $[SiW_{11}CuO_{39}]_n^{6n-}$ chain running along the [010] direction. The condensation process can be viewed as the result of substitution of a water molecule of a $[SiW_{11}O_{39}Cu(OH_2)]^{6-}$ ion by the terminal oxygen atom (O11) on a W center (W11) belonging to an adjacent Keggin unit (Figure 2). The Cu1-O11-W11 angle is equal to 158.1°. This chain-like arrangement is similar to those structures of manganese, cobalt and copper monosubstituted POM salts mentioned above, but obtaining information about the W-O-TM angle is hampered by the crystallographic disorder in the position of the transition metal inside the POM present in most compounds. However, the link in this case can clearly be determined because the copper atom is perfectly located in one position, with W11–O11 (1.75 Å) and Cu1–O11 (2.25 Å), a feature observed only in one of the cobalt derivatives.[9]

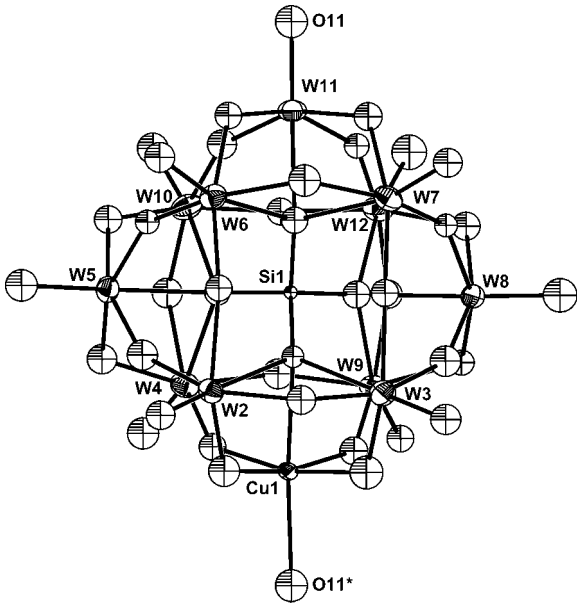

Figure 1. ORTEP view of $[SiW_{11}CuO_{39}]^{6-}$ anion with atom labeling.

The oxygen atoms connected to W atoms can be classified into four groups: O_t terminal oxygen atoms bonded to only one W atom [d(W–O_t) 1.67–1.77 Å], O_c which connect edge-sharing WO_6 octahedra in W_3O_{13} trimers [d(W–O_c) 1.77–2.06 Å], O_b bridging oxygen atoms located in the shared corners between two different W_3O_{13} trimers [d(W–O_b) 1.80–2.04 Å], and O_a coordinated to four M atoms and a Si atom [d(W–O_a) 2.31–2.63 Å]. Relevant bond lengths are displayed in Table 1. The Jahn–Teller effect associated with an octahedral copper(II) ion (Cu1) in the POM induces an elongation of the whole Keggin anion along the chain direction, in spite of a shortening in the metallic framework.

In the cationic complexes the copper(II) ion (Cu2) has a distorted pentacoordinated environment formed by three nitrogen atoms from the tridentate amine coordinated in *mer* fashion, with $\lambda\delta$ conformation, and two oxygen atoms from the bidentate acetate ligand (Figure 3). Experimental and calculated bond lengths and angles are listed in Table 2.

The crystal packing of this compound can be viewed as stacking along the [100] direction of hydrogen-bonded chiral double-chains, each formed by two 2_1 axis related chains linked by the potassium cations K1 and K2 and water molecules through an extended hydrogen-bond network (Figure 4). The two-dimensional arrangement of POM double chains generates a region at $z = {}^1/_2$ where the cationic complexes are settled, which are connected to the POM chain through both acetate oxygen atoms; O41 connects by

Table 1. W–O and Si–O bond lengths [Å] in the $[SiW_{11}CuO_{39}]^{6-}$ polyanion.

Cu1		W2		W3		W4	
O11	2.25(1)	O2	1.68(1)	O3	1.76(2)	O4	1.72(1)
O13	1.98(2)	O13	1.80(1)	O14	1.91(2)	O16	1.77(1)
O15	2.01(2)	O14	1.95(1)	O15	1.81(2)	O22	1.96(1)
O16	1.96(2)	O17	1.91(2)	O19	2.02(2)	O27	1.93(2)
O21	1.98(1)	O18	2.06(1)	O20	1.92(2)	028	2.03(2)
O37	2.40(1)	O37	2.28(1)	O37	2.63(1)	038	2.39(2)
W5		W6		W7		W8	
O5	1.71(1)	O6	1.77(1)	O7	1.67(2)	O8	1.69(1)
O17	1.90(1)	O18	1.84(1)	O19	1.90(2)	O20	1.92(1)
O22	1.93(1)	O23	1.88(1)	O24	1.93(2)	O25	1.88(1)
O23	1.91(1)	O24	1.94(2)	O25	1.96(1)	O26	1.93(1)
O29	1.92(1)	O30	1.92(1)	O31	1.91(1)	O32	1.91(1)
O38	2.311(8)	O39	2.35(1)	O39	2.34(1)	O40	2.329(9)
W9		W10		W11		W12	
O9	1.74(1)	O10	1.72(1)	O11	1.75(2)	O12	1.72(2)
O21	1.79(1)	O28	1.89(2)	O30	1.91(1)	O32	1.96(2)
O26	1.92(1)	O29	1.93(1)	O31	1.94(1)	O33	1.87(2)
O27	1.89(2)	O34	1.93(1)	O34	1.87(2)	O35	1.93(1)
O33	2.04(2)	O36	1.89(1)	O35	1.91(1)	O36	1.90(2)
O40	2.38(1)	O38	2.37(1)	O39	2.27(1)	O40	2.36(1)
Si1							
O37	1.643(4)						
O38	1.631(3)						
O39	1.652(4)						
O40	1.640(4)						

means of hydrogen bonds with water molecules and O42 forming part of coordination sphere of the K4 cation.

Magnetic properties and electronic paramagnetic resonance: The compound presents a magnetic behaviour that fits the Curie–Weiss rule, with an intersection temperature of −1.5 K and a Curie constant value of 0.85 $cm^3 K mol^{-1}$. The negative value of χ and the decrease of $\chi_m T$ from 0.85 to 0.79 with the decrease of temperature are indicative of weak antiferromagnetic interactions. The interactions between the two types of copper atoms present in the structure appear to be of the same magnitude. The effective magnetic moment at room temperature is 2.61 $cm^3 K mol^{-1}$ and decreases weakly when the temperature drops as a result of the weak interactions. Considering the large exchange pathway that separates the different copper atoms this weakness of the magnetic interactions is easily comprehensible.

The X band EPR spectra of the polycrystalline samples of the title compound are shown in Figure 5. The spectra show wide and complex signals with little information as a consequence of the presence of two types of copper(II), which show interactions of the same magnitude and remain unchanged over the range 4–300 K. The decrease of the temperature produces an increase of the signal intensity, which is in agreement with the weakly antiferromagnetic behaviour.

The Q band EPR spectra of the polycrystalline powdered samples at room temperature and at 120 K have been recorded. The presence of the signals corresponding to the two copper ions can be observed in both spectra. One signal shows clear axial symmetry with 10500 and 11700 Gauss

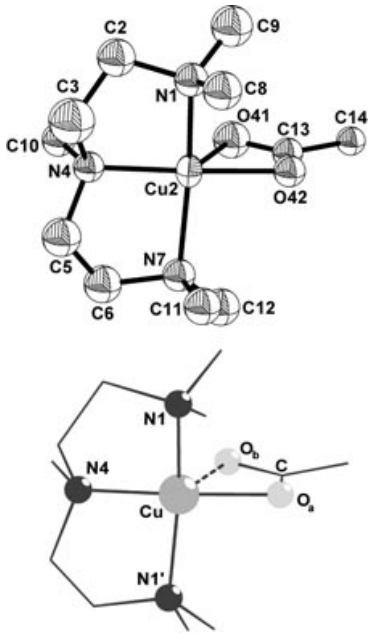

Figure 3. Top: ORTEP view of the [Cu(ac)(pmdien)]$^+$ cationic complex. Bottom: Atom numbering in the [Cu(ac)(dien)]$^+$ cationic model used in DFT calculations.

Table 2. Selected experimental and theoretical (B3LYP optimizations) bond lengths [Å] and angles [°] for cationic complexes.

Experimental		DFT calculations		
	[Cu(ac)(pmdien)]$^+$		[Cu(ac)(pmdien)]$^+$	[Cu(ac)(dien)]$^+$
Cu–N1	2.034	Cu–N1	2.124	2.078
Cu–N4	1.951	Cu–N4	2.063	2.064
Cu–N7	2.039	Cu–N1′	2.124	2.078
Cu–O41	2.358	Cu–O_b	2.307	2.292
Cu–O42	1.971	Cu–O_a	1.972	1.962
N1-Cu-N4	87.23	N1-Cu-N4	86.02	84.07
N1-Cu-N7	154.86	N1-Cu-N1′	150.75	156.54
N1-Cu-O41	102.39	N1-Cu-O_b	104.51	101.60
N1-Cu-O42	94.44	N1-Cu-O_a	95.39	96.90
N4-Cu-O41	112.48	N4-Cu-O_b	112.42	112.67
N4-Cu-O42	171.99	N4-Cu-O_a	173.70	174.33
N7-Cu-O41	102.83	N1′-Cu-O_b	104.51	101.60
N7-Cu-O42	94.72	N1′-Cu-O_a	95.39	96.90
O41-Cu-O42	59.51	O_b-Cu-O_a	61.28	61.66
Cu-O42-C	98.58	Cu-O_a-C	96.56	96.38
		σ(dist)[a]	0.076	0.069
		σ(ang)[a]	2.20	2.22

[a] Root mean square deviation.

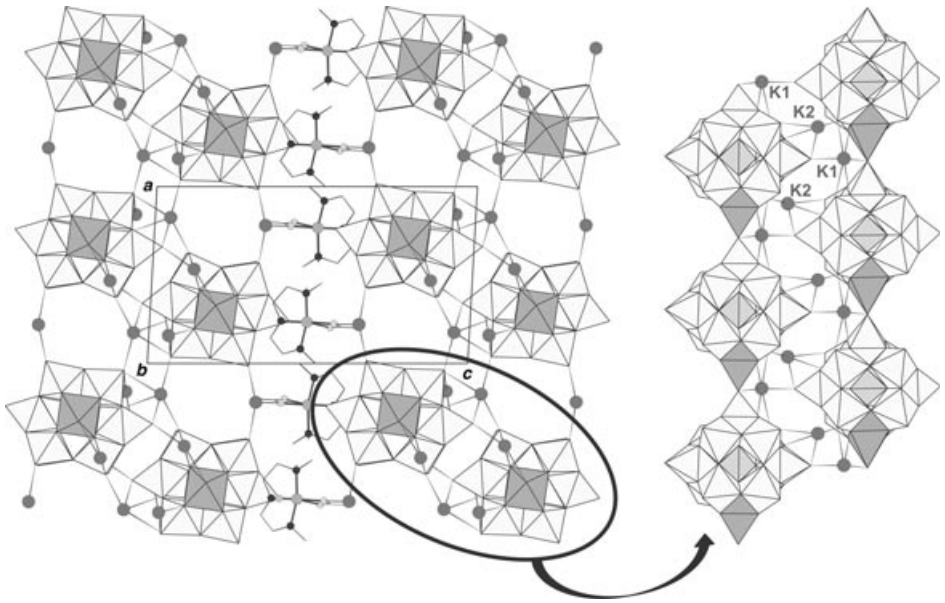

Figure 4. Left: View of crystal packing along the [010] direction. Right: Detailed view of two 2_1-axis-related chiral chains. Water molecules have been omitted for clarity.

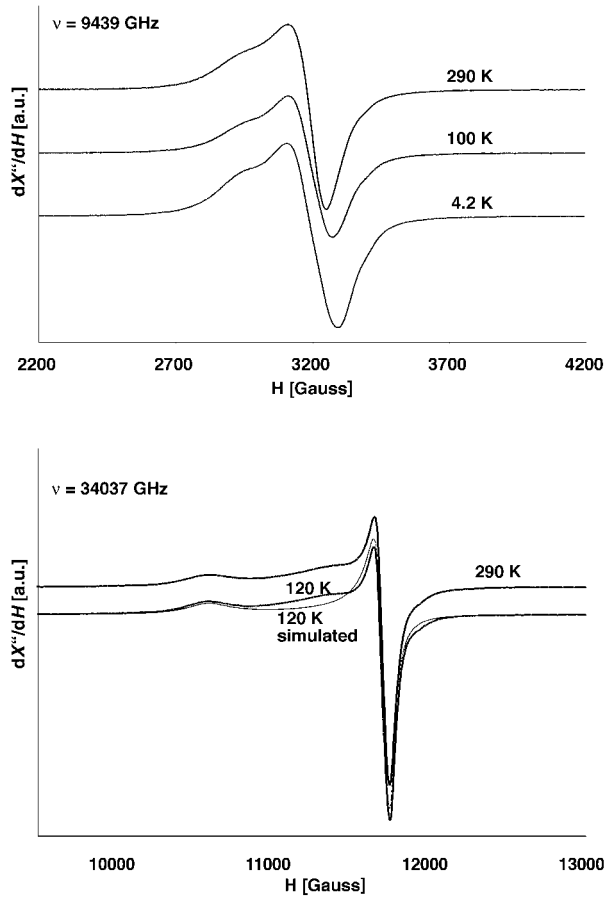

Figure 5. Top: Temperature dependence from 4.2 K up to 290 K of the powder X band EPR spectra. Bottom: Q band EPR powder spectra at 120 and 290 K.

values for $H_{\parallel}$ and $H_{\perp}$, respectively. The second signal is partially masked by the first one and it is difficult to deduce its symmetry. In addition, neither of the two signals shows the corresponding hyperfine structure, confirming the presence of weak but not negligible magnetic interactions.

The signal with axial symmetry can be simulated by using a Lorentzian-type curve, which indicates that the exchange magnetic interactions predominate over the dipolar interactions. The g values used in the simulation are $g_{\parallel}=2.300$ and $g_{\perp}=2.079$, both usual in slightly distorted octahedral system with fundamental state $d_{x^2-y^2}$.

DFT calculations—[Cu(ac)-(dien)]$^+$ stability study: The coordination polyhedron of the cationic complex is very distorted as a consequence of the presence of the acetate group as a bidentate ligand. In order to establish whether this distortion is due to electronic or packing effects, theoretical calculations were performed on the complete [Cu(ac)(pmdien)]$^+$ and the [Cu(ac)(dien)]$^+$ cationic model complexes (Figure 3). Both structures were fully optimized and, as can be seen in Table 2, the calculations reproduce with acceptable precision the experimental copper ion environment.

Several partial optimisations have been made fixing the Cu-O_a-C angle in the 80–120° range. There is a very broad potential well around the minimum so that considerable variations in this angle produce little variation in the total energy of the molecule. An optimized value for the energy minimum of 96.56° is close to the experimental one (98.58°). Furthermore, the angle variation yields a strong change in the copper apical oxygen length and the existence of a bond between both atoms has been questioned. In this context, the AIM theory has been used to determine the relationship between the Cu-O_a-C angle and the acetate ligand denticity. The electronic density maps and associated critical points of the structures corresponding to 85, 97, 102, 103, 104 and 110° values for Cu-O_a-C angle are shown in Figure 6. As can be seen, the Cu–O_b bond breaks at an angle slightly higher than 103°. In this range the BCP and the RCP annihilate each other, and a degenerate critical point of rank 2 appears in their position. This is signaled by a very high value of the ellipticity (ε), which tends to infinity as both critical points approach each other. This kind of degenerate critical point is characteristic of frontier structures between two stable ones. In this case, the two stable structures correspond to the pentacoordinated and tetracoordinated copper(II) atoms. The lack of the Cu–O_b bond critical point (BCP) and the ring critical point (RCP) of the system copper/acetate when the angle is 104° implies tetracoordination of the metallic atom. Hence, the acetate anion acts as a bidentate ligand until the Cu-O_a-C angle reaches a value between 103 and

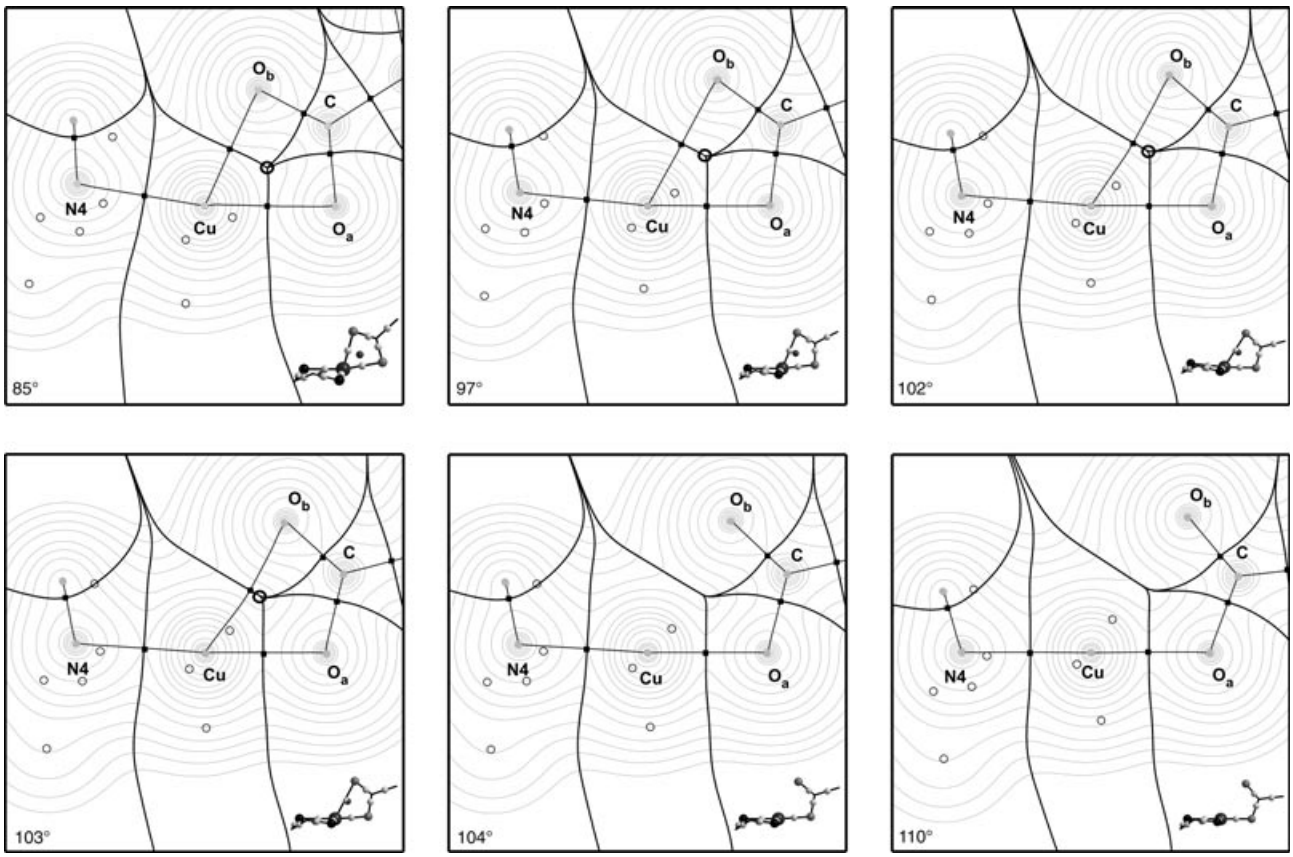

Figure 6. Molecular graph determined by the topology of the electron density in the plane containing the copper atom and the acetate ligand for optimized structures corresponding to 85, 97, 102, 103, 104 and 110° values for the Cu-O_a-C angle. Positions of the bond and angle CPs are denoted by filled squares and bold open circles, respectively.

104°. Table 3 summarizes the geometries and topological properties of the electron density in the cationic model complexes.

A significant destabilization of the molecule has not been observed, in spite of the loss of energy associated with bond breaking, due to reorganization in the rest of the molecule. This can be seen mainly in the shortening of the Cu–O_a bond and a shift of the copper atom to the dien plane as the Cu-O_a-C angle increases. Furthermore, the coordination of the copper ion changes from a very distorted square pyramid to a square plane. The strengthening of the Cu–O_a bond is also noticeable in the increasing values of the electron density (ρ) and its Laplacian ($\nabla^2\rho$) at the bond critical point (Table 3).

Polyhedral distortion: The $[SiW_{11}CuO_{39}]^{6-}$ polyanion in compound **1** is built up from twelve MO_6 distorted octahe-

Table 3. Geometries and topological properties of the electron density at the critical points of the $[Cu(ac)(dien)]^+$ cationic model complexes.

Geometrical parameters[a]						Electron density parameters[b]						
Cu-O_a-C	Cu–O_a	Cu–O_b	Cu–N1	Cu–N4	Cu–dien	ρ Cu–O_a	ρ Cu–O_b	ρ ring	$\nabla^2\rho$ Cu–O_a	$\nabla^2\rho$ Cu–O_b	ε Cu–O_a	ε Cu–O_b
80	2.200	1.951	2.098	2.059	0.843	5.17	9.00	4.49	18.08	46.93	16.25	3.00
85	2.095	2.051	2.095	2.059	0.623	6.49	7.15	4.59	25.41	34.34	0.33	0.26
87	2.062	2.085	2.092	2.060	0.592	6.97	6.62	4.55	28.55	30.55	2.34	1.67
90	2.022	2.145	2.086	2.061	0.526	7.66	5.83	4.40	32.83	25.01	4.88	4.75
92	2.001	2.189	2.083	2.062	0.476	8.06	5.32	4.26	35.36	21.65	5.91	7.89
95	1.973	2.258	2.080	2.062	0.418	8.62	4.62	4.00	38.92	17.45	6.93	15.50
97	1.957	2.307	2.078	2.062	0.395	8.96	4.20	3.81	41.12	15.22	7.39	24.18
100	1.937	2.385	2.075	2.063	0.357	9.40	3.61	3.48	43.96	12.59	7.73	53.06
102	1.927	2.441	2.073	2.062	0.321	9.64	3.26	3.23	45.49	11.37	7.74	122.62
103	1.922	2.469	2.072	2.063	0.303	9.75	3.10	3.10	46.18	11.06	7.71	361.30
104	1.918	2.498	2.070	2.064	0.283	9.84			46.76		7.67	
106	1.911	2.556	2.068	2.064	0.250	10.03			47.98		7.53	
108	1.904	2.614	2.066	2.064	0.223	10.20			49.08		7.35	
110	1.898	2.672	2.066	2.065	0.198	10.33			50.00		7.15	
120	1.876	2.950	2.063	2.063	0.127	10.79			53.73		6.05	

[a] Bond angles [°], bond lengths [Å]; Cu–dien: distance from Cu to mean plane of N dien atoms [Å]. [b] ρ electron density (a.u. $Å^{-3}\times100$); $\nabla^2\rho$ Laplacian of the electron density (a.u. $Å^{-5}\times100$); ε ellipticity ($\times100$).

dra (11 WO_6 and 1 CuO_6) without any disorder in the metallic positions. To quantify the degree of distortion of the different polyhedra continuous shape measures (CSM)[13] have been employed. The CSM determines the normalized distance of a structure from a given reference shape. In the case of our polyanion, the octahedron and the trigonal prism were chosen as reference shapes. The calculations of the continuous shape measure of the coordination sphere of polyanion metallic centers were performed by using the formula proposed in the literature.[14] Table 4 summarizes the shape measures obtained for the W and Cu centers in the $[SiW_{11}CuO_{39}]^{6-}$ polyanion. All centers show $S(O_h)$ values less than 2, which indicates a prevalence of the octahedral geometry. The analysis of the experimental structural data for hexacoordinated tungsten atoms shows that in a scatterplot of the octahedral and trigonal prismatic measures, most polyhedra are located between the lines corresponding to an axial bending of two *trans* ligands and the *trans* effect (see Supporting Information). On the other hand, the copper atom values are located between the lines corresponding to an axial bending of two *trans* ligands and the Jahn–Teller effect.

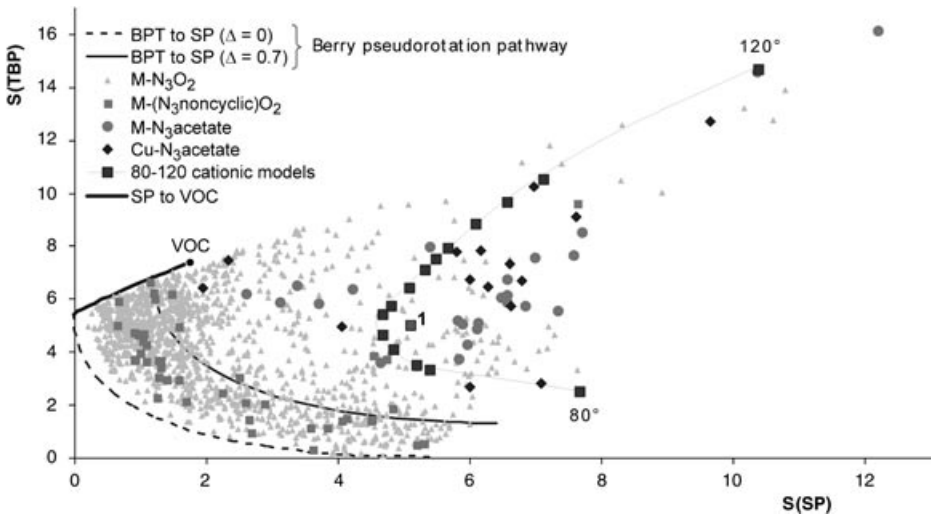

Figure 7. Position in a shape map of the structures of pentacoordinated first series transition metal complexes with an environment MN_3O_2. Square marked as 1 corresponds to the cationic complex in the title compound. Δ means the difference between axial and equatorial bond lengths.

In addition, a distortion study has been carried out with the experimental and model cationic copper complexes together with all pentacoordinated first series transition metal complexes with an MN_3O_2 environment retrieved from the Cambridge Structural Database.[15] The trigonal bipyramid (TBP) and the square pyramid (SP) were used as reference shapes in the CSM calculations for this group of pentacoordinated complexes and Figure 7 displays the corresponding scatterplot of the S(TBP) vs S(SP) shape measures. As can be seen in Table 5, both the experimental cationic complex and the models show high values ($S > 3$)[16] in the shape measures indicating a strong distortion in their geometries. Besides, CSM calculations for a four-coordinated view of the complexes indicate also a strong distortion at low angles. However, the CSM value for a square becomes less than 1 when the angle is higher than 104° where the copper coordination number changes from 5 to 4. This fact confirms the shift of copper ion towards the basal plane as the Cu-O_a-C angle increases.

Table 4. Shape measures for hexacoordinated metallic centers in $[SiW_{11}CuO_{39}]^{6-}$ polyanion[a]

Metallic center	S(OC-6)	S(TPR-6)	Angular distortion[b]
W2	0.79	14.90	0.98
W3	0.80	14.30	0.80
W4	1.12	14.24	1.26
W5	0.86	14.60	1.00
W6	1.20	14.60	1.24
W7	1.07	14.56	1.18
W8	1.00	15.05	1.08
W9	1.18	14.80	1.15
W10	1.04	14.72	1.12
W11	1.10	14.75	1.28
W12	1.02	14.77	1.16
Cu1	1.55	14.72	

[a] OC-6: octahedron; TPR-6: trigonal pyramid. [b] Angular distortion obtained by using the formula: $\Delta_\alpha = \frac{1}{3}\sum_i \left[\frac{\alpha_i - 180}{180}\right]^2$; α_i = O-W-O_{trans}.

Table 5. Shape measures for penta and tetracoordinated $[Cu(ac)(dien)]^+$ model complexes.[a]

Cu-O_a-C angle [°]	S(SPY-5)	S (TBPY-5)	S(SW-4)[b]	S(SP-4)[b]
80	7.67	2.53	4.93	7.75
85	5.40	3.31	8.01	3.94
87	5.19	3.50	8.51	3.58
90	4.84	4.08	9.64	2.80
92	4.68	4.66	10.58	2.25
95	4.68	5.44	11.68	1.73
97	4.81	5.75	12.03	1.62
100	5.07	6.41	12.70	1.39
102	5.33	7.13	13.43	1.14
103	5.48	7.54	13.84	1.01
104	5.66	7.94	14.22	0.91
106	6.08	8.82	14.98	0.72
108	6.57	9.68	15.63	0.59
110	7.12	10.53	16.21	0.50
120	10.38	14.69	18.22	0.31
98.58[c]	*5.10*	*5.02*		

[a] SPY-5: square pyramid; TBPY-5: trigonal bipyramid; SW-4: sawhorse; SP: square. [b] Coordination sphere is formed by the three N dien atoms and the O_a acetate atom. [c] Experimental complex values.

Conclusion

The reaction between a copper monosubstituted Keggin POM and $[Cu(ac)(pmdien)]^+$ generated in situ in aqueous solution affords a hybrid inorganic–metalorganic compound

with a two-dimensional structure consisting of alternated inorganic POM and copper complex layers. The POM layer contains chiral double chains of $[SiW_{11}CuO_{39}]^{6-}$ anions held together by a hydrogen-bonding network involving the water molecules and potassium cations.

Magnetic studies of the compound indicate the presence of weak antiferromagnetic interactions. The Q band EPR spectra of polycrystalline samples display the signals corresponding to the two copper ions. One signal shows clearly axial symmetry, while the second signal is partially masked by the first one, which makes it difficult to deduce its symmetry. The lack of hyperfine structure in both signals confirms the presence of weak but not negligible magnetic interactions.

The relationship between the Cu-O_a-C angle and the acetate denticity was determined by AIM theory calculations by using the $[Cu(ac)(dien)]^+$ cationic models. The study concludes that the acetate anion acts as a bidentate ligand until the Cu-O_a-C angle reaches a value between 103 and 104°.

Polyhedral distortion studies have been carried out by using CSM over the polyanion and copper complexes. The analysis for $[SiW_{11}CuO_{39}]^{6-}$ anion shows that the distortion values in most W polyhedra are located between an axial bending of two *trans* ligands and the *trans* effect; while, the copper distortion value fits between an axial bending of two *trans* ligands and the Jahn–Teller effect. All MO_6 polyhedra show significant deviations from the Bailar pathway. There is a good correlation between the angular distortion and the CSM data for the tungsten centers. This fact confirms that polyhedral distortions are strongly affected by the variation in the angles.

In the case of pentacoordinated cationic complexes, both the experimental and the models show a strong distortion in their geometries. This is due to the low value of the acetate ligand bite angle, which shifts acetate complexes away from the Berry pseudorotation pathway. CSM calculations for a four-coordinated view of the complexes indicate values less than 1 for a square geometry when the Cu-O_a-C angle is higher than 104°, and as the angle increases the geometries tend asymptotically towards the upper limit of the experimental points, which corresponds to a combination of the apical elongation and displacement of the metallic ion to the basal plane of the square pyramid. Finally, the distortion of the $[Cu(ac)(pmdien)]^+$ cation is close to the corresponding theoretical value indicating a low influence of the packing in its geometry.

Experimental Section

Materials: Sodium tungstate dihydrate ($Na_2WO_4{\cdot}2H_2O$, Aldrich), sodium silicate (Na_2SiO_3, Panreac), copper chloride dihydrate ($CuCl_2{\cdot}3H_2O$, Merck), copper nitrate trihydrate ($Cu(NO_3)_2{\cdot}3H_2O$, Fluka), potassium acetate (KCH_3CO_2, Aldrich), *N*,*N*,*N*′,*N*″,*N*″-pentamethyldiethylentriamine ($C_9H_{23}N_3$, Fluka), 37% hydrochloric acid (HCl, Riedel-de-Häen), and methanol (CH_3OH, Riedel-de-Häen) were used as purchased without further purification. The compound $K_8[\alpha\text{-}SiW_{11}O_{39}]$ was prepared according to the literature method.[17]

Methods: IR spectra for solid samples were obtained as KBr pellets on a Mattson 1000 FT-IR spectrometer. Thermogravimetric analysis (TGA) and differential thermal analysis (DTA) were carried on a TA Instruments SDT 2960 thermobalance under a 100 mL min^{-1} flow of synthetic air; the temperature was ramped from 20 to 845 °C at a rate of 5 °C min^{-1}. This instrument was connected, by means of a thermostated line, to a mass spectrometer (Thermostar, Balzers Instruments). The magnetic susceptibility was measured on a Quantum Design MPMS-7 SQUID magnetometer (T range: 5–300 K; applied field: 0.1 T; diamagnetic corrections estimated from Pascal's constants). EPR powder spectra were recorded on a Bruker ESP300 spectrometer (X and Q bands) equipped with Oxford low temperature devices (magnetic field calibration: NMR probe; determination of the frequency inside the cavity: Hewlett-Packard 5352B microwave frequency counter; maintenance of the crystal structures powder samples was confirmed by powder X-ray diffraction; computer simulation: WINEPR-Simfonia, version 1.5, Bruker Analytische Messtechnik GmbH). Carbon, nitrogen and hydrogen were determined by organic microanalysis on a LECO CHNS 932 analyzer.

Synthesis of $K_5[Cu(ac)(pmdien)][SiW_{11}CuO_{39}]{\cdot}12H_2O$ (1): A solution of $CuCl_2{\cdot}2H_2O$ (34 mg, 0.2 mmol), $K_8[\alpha\text{-}SiW_{11}O_{39}]$ (644 mg, 0.2 mmol) and excess potassium acetate in water (40 mL) was heated to 100 °C for 1 h. A solution containing $Cu(NO_3)2{\cdot}H_2O$ (96 mg, 0.2 mmol), *N*,*N*,*N*′,*N*″,*N*″-pentamethyldiethylentriamine (7 mL of a 0.05 M solution in methanol) and excess of potassium acetate in water (30 mL) was added and a blue precipitate formed. The mixture was stirred overnight, and then the precipitate was removed by filtration. Prismatic blue single crystals were obtained from the mother liquor by slow evaporation. Elemental analysis calcd (%) for $C_{11}H_{26}Cu_2K_5N_3O_{41}SiW_{11}{\cdot}12H_2O$: C 3.83, H 1.46, N 1.22; found C 3.81, H 1.38, N 1.23; IR (KBr pellets): $\tilde{\nu}$1010 (w), 954 (s), 902 (vs), 800 (vs), 696 (s), 526 cm^{-1} (m).

Crystal structure analysis: Crystal structure data for compound **1** are summarized in Table 6. Intensity data were collected at room temperature on an Xcalibur single-crystal diffractometer (graphite monochromated $Mo_{K\alpha}$ radiation, $\lambda = 0.71073$ Å, fitted with a Sapphire CCD detector. A total of 1372 frames of data were collected with an exposure time of 20 s per frame by using the ω scan technique with frame width of $\Delta\omega = 0.30°$. Data frames were processed (unit cell determination, intensity data integration and correction for Lorentz and polarization effects) by using the CrysAlis software package.[18] The structure was solved by using Patterson methods (SIR97)[19] and refined by full-matrix least-squares analysis by using the SHELXL-97 program.[20] Thermal vibrations were treated anisotropically for W, Cu, and K atoms only. All pmdien H atoms were included in calculated positions and treated as riding atoms by using default SHELXL parameters. Based on the unusual size of the displacement parameters of atoms K3 and O49 in the refinement under full occupancy, it was decided that the potassium cation and water molecule were disordered over both positions. Therefore, the site occupancies were refined resulting in an occupancy ratio 66.5:33.5 for the potassium atom. All calculations were performed by using the WinGX crystallographic software package[21] running on a PC. The final geometrical calculations and the graphical manipulations were carried out with the PLATON program.[22]

CCDC-234031 contains the supplementary crystallographic data for this paper. This data can be obtained free of charge from www.ccdc.cam.ac.uk/conts/retrieving.html (or from the Cambridge Crystallographic Data Centre, 12 Union Road, Cambridge CB21EZ, UK; fax: (+44) 1223-336-033; or deposit@ccdc.cam.uk).

Computational details: All the quantum calculations of geometric optimization of the coordination compounds and sunsequently obtaining the electronic density have been carried out by using the Gaussian98 program.[23] The topological analysis of this electronic density has been made with MORPHY98 program.[24] Both programs have run on computers with a GNU/Linux operating system.

A C_s ideal symmetry and a doublet state ($S = {}^1/_2$) have been imposed in all calculations of the coordination compounds. Density functional theory and specifically Becke's hybrid method with three parameters[25] based on nonlocal exchange and correlation functionals, as implemented in Gaussian98 (B3LYP), has been used. The standard 6-311+G(d)[26] basis has been chosen for all atoms. This basis contains diffuse[27] and polarization[28] functions for all atoms, except hydrogen. The single crystal experi-

Table 6. X-ray crystallographic data for $K_5[Cu(ac)(pmdien)][SiW_{11}CuO_{39}]\cdot 12H_2O$.

formula	$C_{11}H_{50}Cu_2K_5N_3O_{53}SiW_{11}$
M_w [g]	3445.53
crystal system	monoclinic
space group	$P2_1$
T [K]	293(2)
a [Å]	12.467(5)
b [Å]	10.897(5)
c [Å]	22.452(5)
β [°]	93.220(5)
V [Å^3]	3045(2)
Z	2
μ [mm^{-1}]	21.825
ρ_{calcd} [g cm^3]	3.679
θ limits [°]	3–29.5
reflections measured	22228
unique reflns (R_{int})	12246 (0.037)
observed reflns [$I>2\sigma(I)$]	7316
absorption correction	analytical (min. 0.122, max. 0.652)
refined parameters	437
$R(F_o)$[a]	0.0403
$Rw(F_o^2)$[a] (all data)	0.0768
Flack Parameter	0.10(1)

[a] $R(F)=\Sigma||F_o|-|F_c||/\Sigma|F_o|$, $Rw(F^2)=\{\Sigma[w(F_o^2-F_c^2)^2]/\Sigma[w(F_o^2)]\}^{1/2}$.

mental data were used as a starting point in the global optimizations of $[Cu(ac)(pmdien)]^+$ and $[Cu(ac)(dien)]^+$ model compounds without any type of restriction. As the methyl groups of pmdien ligand do not have a significant influence on the geometry, the $[Cu(ac)(dien)]^+$ cationic model has been used for the partial optimization of the $[Cu(ac)(dien)]^+$ model, with the Cu-O-C angle restricted in the range 80–120° in order to reduce computational time.

The CSM calculations of the different polyhedra have been performed with the program SHAPE v1.1a.[29] The April 2003 release of the Cambridge Structural Database was used in this work to obtain the different WO_6 (559 hits) and CuN_3O_2 (1062 hits) polyhedra. All searches were restricted to those CSD entries that satisfied the following secondary search criteria: a) error-free after CSD evaluation procedures, b) no reported structural disorder and c) perfect matching of their chemical and crystallographic connectivity representations.

Acknowledgements

This work was supported by Universidad del País Vasco (9/UPV 00169.310–15329/2003) and Ministerio de Ciencia y Tecnología (MAT2002–03166). L.S.F. thanks Ministerio de Ciencia y Tecnología.

[1] a) M. T. Pope, A. Müller, *Angew. Chem.* **1991**, *103*, 56; *Angew. Chem. Int. Ed. Engl.* **1991**, *30*, 34; b) *Polyoxometalates: From Platonic Solids to Antiretroviral Activity* (Eds.: M. T. Pope, A. Müller), Kluwer, Dordrecht (The Netherlands), **1994**; d) *Polyoxometalates: From Topology via Self-Assembly to Applications* (Eds.: M. T. Pope, A. Müller), Kluwer, Dordrecht (The Netherlands), **2001**; e) *Polyoxometalate Chemistry for Nanocomposite Design* (Eds.: M. T. Pope, T. Yamase), Kluwer, Dordrecht (The Netherlands), **2002**; f) *Polyoxometalate Molecular Science* (Eds.: J. J. Borrás-Almenar, E. Coronado, A. Müller, M. Pope), Kluwer, Dordrecht (The Netherlands), **2003**.

[2] D. E. Katsoulis, *Chem. Rev.* **1998**, *98*, 359, and references therein.

[3] a) A. Milonas, E. Papaconstantinou, *J. Mol. Catal.* **1994**, *92*, 261; b) A. Corma, *Chem. Rev.* **1995**, *95*, 559; c) I. V. Kozhevnikov, *Catal. Rev. Sci. Eng.* **1995**, *37*, 311; d) I. A. Weinstock, *Chem. Rev.* **1998**, *98*, 113; e) I. V. Kozhevnikov, *Chem. Rev.* **1998**, *98*, 171; f) N. Mizuno, M. Misono, *Chem. Rev.* **1998**, *98*, 199; g) R. Neumann, *Prog. Inorg. Chem.* **1998**, *47*, 317; g) M. Misono, *Chem. Commun.* **2001**, 1141; A. M. Khenkin, L. Weiner, Y. Wang, R. Neumann, *J. Am. Chem. Soc.* **2001**, *123*, 8531.

[4] a) E. Coronado, C. J. Gómez-García, *Comments Inorg. Chem.* **1995**, *17*, 255; b) E. Coronado, C. J. Gómez-García, *Chem. Rev.* **1998**, *98*, 273; c) T. Yamase, *Chem. Rev.* **1998**, *98*, 307; d) L. Ouahab, *Coord. Chem. Rev.* **1998**, *178*, 1501; e) E. Coronado, J. R. Galán-Mascarós, C. Giménez-Saiz, C. J. Gómez-García, *Adv. Mater. Opt. Electron.* **1998**, *8*, 61; f) J. M. Clemente-Juan, E. Coronado, *Coord. Chem. Rev.* **1999**, *193*, 361; g) M. Clemente-León, E. Coronado, P. Delhaes, C. J. Gómez-García, C. Mingolaud, *Adv. Mater.* **2001**, *13*, 574.

[5] a) C. L. Hill, M. S. Weeks, R. F. Schinazi, *J. Med. Chem.* **1990**, *33*, 2767; b) Y. Inouye, Y. Tale, Y. Tokutake, T. Yoshida, A. Yamamoto, T. Yamase, S. Nakamura, *Chem. Pharm. Bull.* **1990**, *38*, 285; c) J. T. Rhule, C. L. Hill, D. A. Judd, R. F. Schinazi, *Chem. Rev.* **1998**, *98*, 327; d) N. Fukuda, T. Yamase, Y. Tajima, *Biol. Pharm. Bull.* **1999**, *22*, 463.

[6] a) D. Hagrman, P. J. Zapf, J. Zubieta, *Chem. Commun.* **1998**, 1283; b) D. Hagrman, P. J. Hagrman, J. Zubieta, *Angew. Chem.* **1999**, *111*, 3359; *Angew. Chem. Int. Ed.* **1999**, *38*, 3165; c) L.-M. Zheng, T. Whitfield, X. Wang, A. J. Jacobson, *Angew. Chem.* **2000**, *112*, 4702; *Angew. Chem. Int. Ed.* **2000**, *39*, 4528; d) J. Do, A. J. Jacobson, *Inorg. Chem.* **2001**, *40*, 598; e) P. J. Hagrman, J. Zubieta, *Inorg. Chem.* **2001**, *40*, 2800; f) L.-M. Zheng, X. Wang, Y. Wang, A. J. Jacobson, *J. Mater. Chem.* **2001**, *11*, 1100; g) R. L. Laduca, Jr., R. S. Rarig, Jr., J. Zubieta, *Inorg. Chem.* **2001**, *40*, 607; h) C.-Z. Lu, C.-D. Wu, H.-H. Zhuang, J.-S. Huang, *Chem. Mater.* **2002**, *14*, 2649; i) R. Nandini Devi, J. Zubieta, *Inorg. Chim. Acta* **2002**, *332*, 72; j) R. C. Finn, J. Sims, C. J. O'Connor, J. Zubieta, *J. Chem. Soc. Dalton Trans.* **2002**, 159.

[7] E. Burkholder, V. Golub, C. J. O'Connor, J. Zubieta, *Inorg. Chem. Commun.* **2004**, *7*, 363.

[8] a) J. R. Galán-Mascarós, C. Giménez-Saiz, S. Triki, C. J. Gómez-García, E. Coronado, L. Ouahab, *Angew. Chem.* **1995**, *107*, 1601; *Angew. Chem. Int. Ed.* **1995**, *34*, 1460; b) E. Coronado, J. R. Galán-Mascarós, C. Giménez-Saiz, C. J. Gómez-García, S. Triki, *J. Am. Chem. Soc.* **1998**, *120*, 4671.

[9] H. T. Evans, T. J. R. Weakley, G. B. Jameson, *J. Chem. Soc. Dalton Trans.* **1996**, 2537.

[10] B. Yan, Y. Xu, X. Bu, N. K. Goh, L. S. Chia, G. D. Stucky, *J. Chem. Soc. Dalton Trans.* **2001**, 2009.

[11] L. Lisnard, A. Dolbecq, P. Mialane, J. Marrot, F. Sécheresse, *Inorg. Chim. Acta* **2004**, *357*, 845.

[12] S. Reinoso, P. Vitoria, L. Lezama, A. Luque, J. M. Gutiérez-Zorrilla, *Inorg. Chem.* **2003**, *42*, 3709.

[13] a) H. Zabrodsky, S. Peleg, D. Avnir, *J. Am. Chem. Soc.* **1992**, *114*, 7843; b) S. Alvarez, M. Llunell, *J. Chem. Soc. Dalton Trans.* **2000**, 3288; c) S. Alvarez, D. Avnir, M. Llunell, M. Pinsky, *New J. Chem.* **2002**, *26*, 996; S. Alvarez, *An. Quim.* **2003**, *99*, 29.

[14] D. Casanova, J. Cirera, M. Llunell, P. Alemany, D. Avnir, S. Alvarez, *J. Am. Chem. Soc.* **2004**, *126*, 1755.

[15] F. H. Allen, *Acta Crystallogr. Sect. B* **2002**, *58*, 380.

[16] H. Zabrodsky, S. Peleg, D. Avnir, *J. Am. Chem. Soc.* **1993**, *115*, 8278; H. Zabrodsky, S. Peleg, D. Avnir, *J. Am. Chem. Soc.* **1994**, *116*, 656.

[17] A. Tézé, G. Hervé, *J. Inorg. Nucl. Chem.* **1977**, *39*, 999.

[18] Oxford Diffraction, CrysAlis CCD and RED. Version 1.70, Oxford Diffraction Ltd, Oxford (UK), **2003**.

[19] A. Altomare, M. C. Burla, M. Camalli, G. Cascarano, G. Luca, C. Giacovazzo, A. Guagliardi, A. G. G. Moliterni, G. Polidori, R. Spagna, *J. Appl. Crystallogr.* **1999**, *32*, 115.

[20] G. M. Sheldrick, SHELXL97, University of Göttingen, Göttingen (Germany), **1999**.

[21] L. J. Farrugia, *J. Appl. Crystallogr.* **1999**, *32*, 837.

[22] A. L. Speck, PLATON, Utrecht University, Utrecht (The Netherlands), **2001**.

[23] Gaussian 98W (Revision A.7), M. J. Frisch, G. W. Trucks, H. B. Schlegel, G. E. Scuseria, M. A. Robb, J. R. Cheeseman, V. G. Zakrzewski, J. A. Montgomery, R. E. Stratmann, J. C. Burant, S. Dapprich, J. M. Millam, A. D. Daniels, K. N. Kudin, M. C. Strain, O. Farkas, J. Tomasi, V. Barone, M. Cossi, R. Cammi, B. Mennucci, C. Pomelli, C. Adamo, S. Clifford, J. Ochterski, G. A. Petersson, P. Y. Ayala, Q. Cui, K. Morokuma, D. K. Malick, A. D. Rabuck, K. Ra-

ghavachari, J. B. Foresman, J. Cioslowski, J. V. Ortiz, B. B. Stefanov, G. Liu, A. Liashenko, P. Piskorz, I. Komaromi, R. Gomperts, R. L. Martin, D. J. Fox, T. Keith, M. A. Al-Laham, C. Y. Peng, A. Nanayakkara, C. Gonzalez, M. Challacombe, P. M. W. Gill, B. G. Johnson, W. Chen, M. W. Wong, J. L. Andres, M. Head-Gordon, E. S. Replogle, J. A. Pople, Gaussian, Inc., Pittsburgh PA, **1998**.

[24] a) P. L. A. Popelier, R. G. A. Bone, MORPHY98, UMIST, Manchester, England, **1998**; b) P. L. A. Popelier, *Comput. Phys. Commun.* **1995**, *93*, 212.

[25] A. D. Becke, *J. Chem. Phys.* **1993**, *98*, 5648.

[26] a) A. J. H. Wachters, *J. Chem. Phys.* **1970**, *52*, 1033; b) P. J. Hay, *J. Chem. Phys.* **1977**, *66*, 4377; c) K. Raghavachari, G. W. Trucks, *J. Chem. Phys.* **1989**, *91*, 1062.

[27] T. Clark, J. Chandrasekhar, G. W. Spitznagel, P. V. R. Schleyer, *J. Comput. Chem.* **1983**, *4*, 294.

[28] M. J. Frisch, J. A. Pople, J. S. Winkley, *J. Chem. Phys.* **1984**, *80*, 3265.

[29] M. Llunell, D. Casanova, J. Cirera, J. M. Bofill, P. Alemany, S. Alvarez, M. Pinsky, D. Avnir, SHAPE v1.1a, Barcelona (Spain), **2003**.

Received: March 22, 2004
Published online: August 24, 2004